arXiv:cond-mat/0101478v1 31 Jan 2001

Stability of exact solutions of the defocusing nonlinear Schrödinger equation with periodic potential in two dimensions

Bernard Deconinck [1], Bela A. Frigyik, J. Nathan Kutz [2]

Department of Applied Mathematics, University of Washington, Seattle, WA 98195-2420

A higher resolution version of this preprint is available at: http://www.amath.washington.edu∼kutz/research.html

Abstract

The cubic nonlinear Schrödinger equation with repulsive nonlinearity and elliptic function potential in two-dimensions models a repulsive dilute gas Bose–Einstein condensate in a lattice potential. A family of exact stationary solutions is presented and its stability is examined using analytical and numerical methods. All stable trivial-phase solutions are off-set from the zero level. Our results imply that a large number of condensed atoms is sufficient to form a stable, periodic condensate.

Key words: Bose-Einstein condensates, two-dimensional nonlinear Schrödinger equation, periodic potential, elliptic functions
PACS: 65.65

1 Introduction

The cubic nonlinear Schrödinger equation with attractive or repulsive nonlinearity and a potential is used as a mean-field model for the dynamics of a dilute-gas Bose Einstein condensate (BEC) [1,2]. In this case, the equation is often referred to as the Gross-Pitaevskii equation. These BECs are of interest in both the theoretical and experimental physics community: they are examples of macroscopic quantum phenomena which display phase coherence [3–6]

[1] Corresponding author (deconinc@amath.washington.edu, phone: (206) 685-2971, fax: (206) 685-1440). Acknowledges support from the National Science Foundation (DMS-0071568).
[2] Acknowledges support from the National Science Foundation (DMS-0092682).

and which have potential applications in such diverse areas as quantum logic [7], matter-wave diffraction [8], and matter-wave transport [9].

After rescaling of the physical variables, the governing equation is

$$i\frac{\partial}{\partial t}\psi(\vec{x},t) = -\frac{1}{2}\Delta\psi(\vec{x},t) + \alpha\left|\psi(\vec{x},t)\right|^2\psi(\vec{x},t) + V(\vec{x})\psi(\vec{x},t), \qquad (1)$$

where Δ denotes the Laplacian operator, $\psi(\vec{x},t)$ is the macroscopic wave function of the condensate in one, two or three dimensions, with $\vec{x}$ defined as x, (x,y) or (x,y,z) respectively. The real-valued function $V(\vec{x})$ is an experimentally generated macroscopic potential. The parameter α determines whether (1) is repulsive ($\alpha = 1$, defocusing nonlinearity), or attractive, ($\alpha = -1$, focusing nonlinearity). Note that for BEC applications, both signs of α are relevant.

Many BEC experiments use harmonic confinement, but recently there has been interest in confinement of repulsive BECs using standing light waves, resulting in a sinusoidal potential in the Nonlinear Schrödinger equation. So far, most interest has focussed on the quasi-one-dimensional regime, in which the longitudinal dimension of the condensate is far greater than the transverse dimensions, which are themselves of the order of the healing length of the condensate. In this case, the governing mean-field equation is (1), with $\alpha = 1$, in one dimension, and the experimentally generated potential $V(x) = -V_0\ \mathrm{sin}^2(x)$. In [10,11], a number of exact solutions of this equation was constructed and their stability was investigated. In fact, a potential more general than a sinusoidal potential was considered:

$$V(x) = -V_0\ \mathrm{sn}^2(x,k), \qquad (2)$$

where $\mathrm{sn}(x,k)$ denotes the Jacobian elliptic sine function, with elliptic modulus k. In the limit $k = 0$, this potential reduces to a sinusoidal potential. It is important to realize that for values of k up to $k = 0.9$, the shape of the potential is virtually indistinguishable from a sinusoidal one. On the other hand, considering values of k close to 1, *i.e.*, $k > 0.999$ gives periodic potentials with well-separated peaks, allowing the study of BEC dynamics in an entirely new regime.

Currently, no experiments are being performed where a BEC is trapped in a higher-than-one-dimensional periodic potential. However, the interest in the applications mentioned above strongly suggests that these experiments may eventually take place. Already, there are theoretical investigations of BECs in multidimensional lattice potentials [12], suggesting the realization of such experiments. Although motivated by the developments in BECs, in this paper

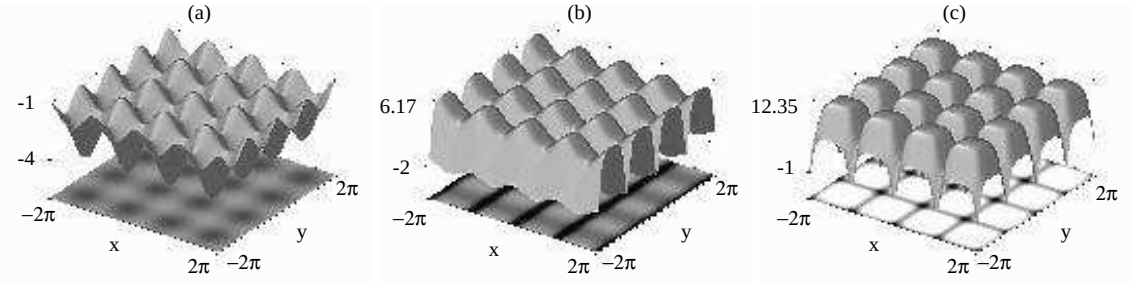

Fig. 1. Various lattice potentials. For all figures, $A_1 = A_2 = B_1 = B_2 = 1$. For (a), $k_1 = k_2 = 0$, $m_1 = m_2 = 1$; for (b), $k_1 = 0.999$, $k_2 = 0$, $m_1 = 2K(0.999)/\pi$, $m_2 = 1$. Finally, for (c) $k_1 = k_2 = 0.999$ and $m_1 = m_2 = 2K(0.999)/\pi$.

we consider (1) with repulsive nonlinearity in two dimensions in its own right. Thus we consider

$$i\frac{\partial\psi}{\partial t} = -\frac{1}{2}\left(\frac{\partial^2\psi}{\partial x^2} + \frac{\partial^2\psi}{\partial y^2}\right) + |\psi|^2\,\psi + V(x,y)\psi, \tag{1$'$}$$

with $\psi = \psi(x, y, t)$. As in one dimension [10,11], making the proper choices for the potential allows the construction of a large class of exact solutions. The family of potentials considered is

$$\begin{aligned} V(x,y) = &-\Big(A_1\mathrm{sn}^2(m_1x,k_1) + B_1\Big)\Big(A_2\mathrm{sn}^2(m_2y,k_2) + B_2\Big) + \\ &+m_1^2k_1^2\mathrm{sn}^2(m_1x,k_1) + m_2^2k_2^2\mathrm{sn}^2(m_2y,k_2). \end{aligned} \tag{3}$$

Here A_1, A_2, B_1, B_2, m_1 and m_2 are real constants. The two elliptic moduli k_1 and k_2 are in the interval $[0, 1]$. The first term is a straightforward generalization of the one-dimensional potential (2), with an additive constant. The other terms are incorporated to facilitate the construction of exact solutions. Although this exact expression for the potential is necessary to allow the construction of exact solutions, it is the qualitative features, *i.e.*, its periodicity and amplitude, that are most important. Numerical and analytical results throughout this paper demonstrate that the behavior of a solution in a lattice potential is largely independent of the quantitative features of the potential. Figure 1 displays the potential (3) for various values of its parameters. In the next section, a family of exact solutions to (1′) is given and their linear stability is discussed. Numerical results for various representative solutions are given in Section 3. The last section concludes the paper with a brief summary of the relevant mathematical and physical results.

2 Analytical Results

A judicious choice of the potential allows for the cancellation of the nonlinear term in (1′) so that exact solutions can be constructed. Of course, one can always find a suitable potential by solving (1′) for $V(x, y)$, given a certain $\psi(x, y, t)$. However, this generically results in time-dependent potentials and is hence not of interest. The kind of potentials we seek are two-dimensional generalizations of the one-dimensional potential (2). This one-dimensional potential is periodic. Its two-dimensional generalizations should be periodic in both its spatial variables. Furthermore, it is desirable that for a given potential more than one exact solution exists.

A derivation of the exact solutions is not presented in this paper. Rather we state the solution formulas and discuss them. For the potential (3), a class of exact solutions is given by

$$\psi(x, y, t) = r_1(x) r_2(y) e^{i\theta_1(x) + i\theta_2(y) - i\omega t}, \tag{4}$$

with

$$r_1^2(x) = A_1 \, \mathrm{sn}^2(m_1 x, k_1) + B_1, \quad \theta_1(x) = c_1 \int_0^x \frac{dz}{A_1 \, \mathrm{sn}^2(m_1 z, k_1) + B_1}, \tag{5a}$$

$$r_2^2(y) = A_2 \, \mathrm{sn}^2(m_2 y, k_2) + B_2, \quad \theta_2(y) = c_2 \int_0^y \frac{dz}{A_2 \, \mathrm{sn}^2(m_2 z, k_2) + B_2}, \tag{5b}$$

and

$$\omega = \frac{1}{2} m_1^2 \left(1 + k_1^2 + k_1^2 \frac{B_1}{A_1}\right) + \frac{1}{2} m_2^2 \left(1 + k_2^2 + k_2^2 \frac{B_2}{A_2}\right), \tag{6a}$$

$$c_1^2 = m_1^2 \frac{B_1}{A_1} (A_1 + B_1) \left(A_1 + k_1^2 B_1\right), \tag{6b}$$

$$c_2^2 = m_2^2 \frac{B_2}{A_2} (A_2 + B_2) \left(A_2 + k_2^2 B_2\right). \tag{6c}$$

Choosing the parameters $A_1 A_2$, B_1/A_1, B_2/A_2, m_1, m_2, k_1 and k_2 determines the potential. Thus the solution class given by (5a-b) is a one-parameter family of solutions, with free parameter A_1/A_2. Existence of these solutions requires $r_1^2 \geq 0, c_1^2 \geq 0$ and $r_2^2 \geq 0, c_2^2 \geq 0$. This imposes conditions on the parameters: $A_i \geq 0, B_i \geq 0$ or $B_i \geq 0, -A_i \leq B_i \leq -A_i/k_i^2$, where $i = 1, 2$.

From (5a-b), it follows that $r_1(x)$ is periodic in x with period $2K(k_1)/m_1$, where $K(k) = \int_0^{\pi/2} dz/\sqrt{1 - k_1^2 \sin^2(z)}$, and $r_2(y)$ is periodic in y with period

$2K(k_2)/m_2$. In general, $\theta_1(x + 2K(k_1)/m_1) \neq \theta_1(x) + 2n\pi$, for some integer n. Thus, the solution (4) is usually not periodic in x or in y. Imposing this periodicity requires a quantization of the phase $\theta_1(x)$ and $\theta_2(y)$ [11]. It is unclear if such a quantization is possible, since only one free parameter is available to satisfy two conditions. There are two special cases in which phase quantization is not a concern. The first case results in trivial-phase solutions, for which $c_1 = 0$, $c_2 = 0$. The second case is the trigonometric limit, in which $k_1 = 0$, $k_2 = 0$.

The solution has trivial phase in the i-direction if c_i is zero, where $i = 1$ (2) corresponds to the x (y)-direction. There are three possibilities:

$$B_i = 0: \qquad r_i = \sqrt{A_i}\ \mathrm{sn}(m_i x, k_i), \tag{7a}$$

$$B_i = -A_i: \qquad r_i = \sqrt{-A_i}\ \mathrm{cn}(m_i x, k_i), \tag{7b}$$

$$B_i = -A_i/k_i^2: \quad r_i = \sqrt{-A_i/k_i^2}\ \mathrm{dn}(m_i x, k_i), \tag{7c}$$

where $\mathrm{cn}(m_i x_i, k_i)$ is the Jacobian elliptic cosine function, and $\mathrm{dn}(m_i x_i, k_i)$ denotes the third Jacobian elliptic function.

The solution is trigonometric in the i-direction if k_i is zero. Then

$$r_i^2(x) = A_i \sin^2(x_i) + B_i, \quad \tan(\theta_i) = \sqrt{1 + \frac{A_i}{B_i}}\tan(m_i x_i), \tag{8}$$

and phase quantization is satisfied. Notice that it is possible for the solution to have trivial phase in one direction and be trigonometric in the other.

The main stability results from [10,11] can be generalized to two dimensions in a straightforward manner. The details of this will be presented elsewhere. Here a brief summary is given. Examining the linear stability of exact trivial-phase stationary solutions $\psi(x, y, t) = r(x, y)\exp(-i\omega t)$ of equation (1′) gives rise to the eigenvalue problem

$$\begin{pmatrix} 0 & -L_- \\ L_+ & 0 \end{pmatrix} \begin{pmatrix} u_1 \\ u_2 \end{pmatrix} = \lambda \begin{pmatrix} u_1 \\ u_2, \end{pmatrix} \tag{9}$$

where the linear Schrödinger operators L_+ and L_- are

$$L_+ = -\frac{1}{2}\left(\partial_x^2 + \partial_y^2\right) + 3r^2(x, y) + V(x, y) - \omega, \tag{10a}$$

$$L_- = -\frac{1}{2}\left(\partial_x^2 + \partial_y^2\right) + r^2(x, y) + V(x, y) - \omega. \tag{10b}$$

Reasoning similar to the arguments in [10,11] leads to the following conclusions:

- If $r(x,y) > 0$, then $r(x,y)$ is the ground state of L_- and $\psi(x,y,t)$ is linearly stable.
- If $r(x,y)$ has any zeros, it is not the ground state of L_-. If in addition L_+ is a positive operator, then $\psi(x,y,t)$ is unstable.
- In all other cases, no conclusion is obtained from this stability analysis.

Primarily, this analysis immediately establishes the linear stability of a solution $\psi(x,y,t) = r_1(x)r_2(y)\exp(-i\omega t)$, where both $r_1(x)$ and $r_2(y)$ are strictly positive. Thus, the solution with both the x- and y-dependence specified by (7c) is linearly stable.

3 Numerical Results

In this section, the result of numerically solving (1′) with initial conditions chosen from the exact solutions given in the previous section are discussed. The numerical procedure uses a fourth-order Runge-Kutta method in time and a filtered pseudospectral method in space. For each experiment, a small amount of white noise was added to the initial conditions as a perturbation.

Consider the solution

$$\psi(x,y,t) = \frac{\sqrt{-A_1}\sqrt{-A_2}}{k_1 k_2}\mathrm{dn}(m_1 x, k_1)\mathrm{dn}(m_2 y, k_2)e^{-i\omega t}. \tag{11}$$

where $A_1 < 0$ and $A_2 < 0$. As stated in the previous section, this solution is linearly stable. This is confirmed by the numerics presented in Fig. 2. The three different columns give from left to right the dynamics of the solution, the same using contour plots, and the arctan of the Fourier power spectrum of the solution. In the first two columns, the bottom figure shows the potential $V(x,y)$. The stability of this solution is reminiscent of the stability of a plane wave solution of the two-dimensional defocusing nonlinear Schrödinger equation [13].

Next, consider the trivial-phase solution

$$\psi(x,y,t) = \sqrt{-A_1}\sqrt{-A_2}\ \mathrm{cn}(m_1 x, k_1)\mathrm{cn}(m_2 y, k_2)e^{-i\omega t}. \tag{12}$$

The numerics of Fig. 3 shows that this solution is unstable. For the equation (1′), the L^2-norm of the solution is conserved, hence so is the L^2-norm of its Fourier spectrum. This is not reflected in Fig. 3, due to the arctan

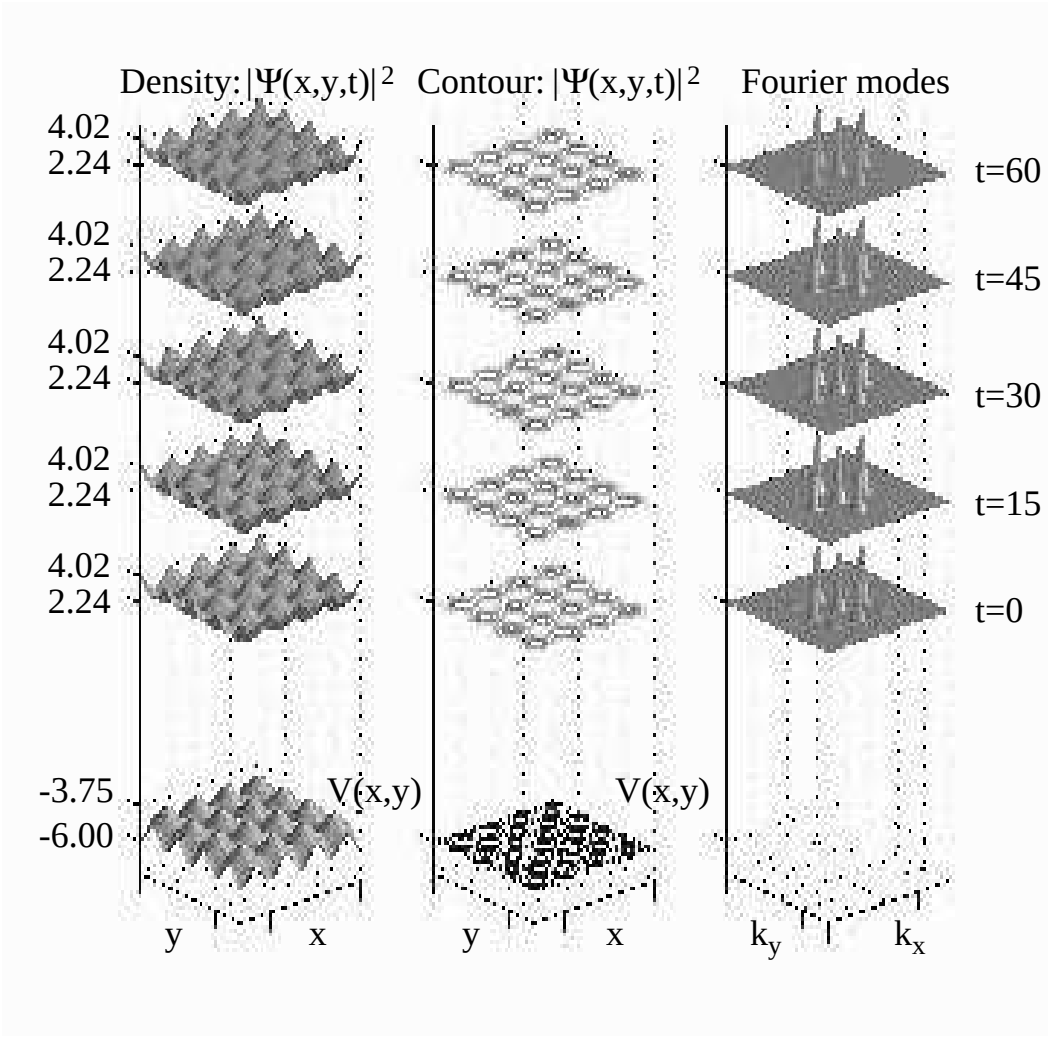

Fig. 2. The stable solution from Eqn. (11). Here $k_1 = k_2 = 1/2$, $m_1 = m_2 = 1$ and $A_1 = A_2 = -1$.

transformation, which is used to diminish the range of the power spectrum. The onset of instability occurs between $t = 15$ and $t = 30$. A detailed look at this onset is given in Fig. 4. The middle column of this figure shows $||\psi(x,y,t)|^2 - |\psi(x,y,t=0)|^2|$. The instability begins to develop around $t = 18$. Before the instability occurs, $|\psi(x,y,t)|^2$ is equal to its initial condition, up to effects due to the added noise and numerical round-off, as is expected, since $\psi(x,y,t)$ is an exact stationary solution of (1′). The solution

$$\psi(x,y,t) = \sqrt{A_1 A_2}\,\mathrm{sn}(m_1 x, k_1)\,\mathrm{sn}(m_2 y, k_2)\,e^{-i\omega t}. \tag{13}$$

is observed numerically to be unstable as well. Its dynamics is very similar to that of the solution (12). These results are consistent with the one-dimensional results obtained previously [10,11].

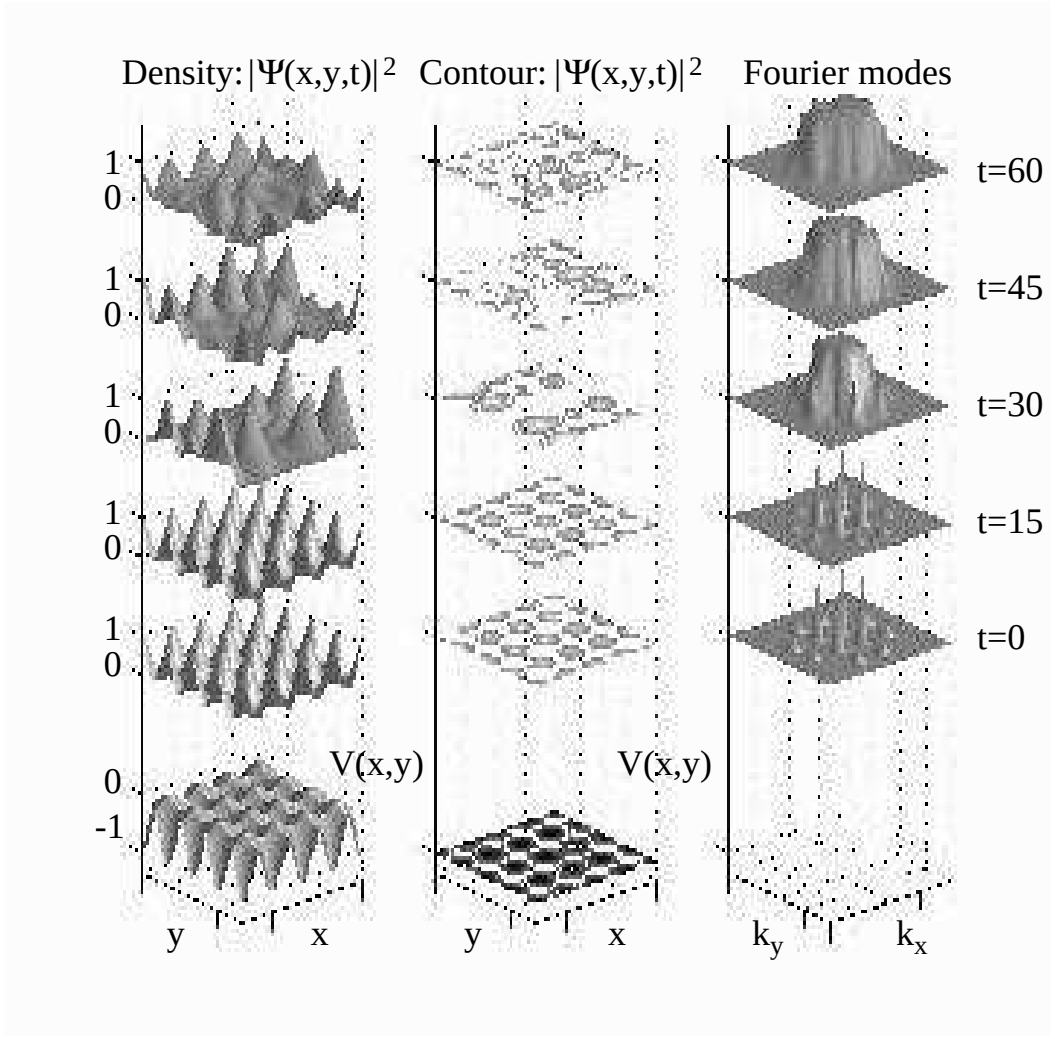

Fig. 3. The unstable solution from Eqn. (12). Here $k_1 = k_2 = 1/2$, $m_1 = m_2 = 1$ and $A_1 = A_2 = 1$.

Analytical results for the stability of the nontrivial phase solutions are difficult to obtain, and so far numerical investigations are the only means of examining these solutions. Since phase quantization is a serious complication for the numerics, it is convenient to work with solutions (8) that are trigonometric in both directions since phase quantization is automatically satisfied. Thus, we consider solutions of the form

$$\psi(x,y,t) = \sqrt{\Big(A_1 \sin^2(m_1 x) + B_1\Big)\Big(A_2 \sin^2(m_2 y) + B_2\Big)}\, e^{i\theta_1(x) + i\theta_2(y) - i\omega t}, \quad (14)$$

with

$$\tan(\theta_1(x)) = \sqrt{1 + \frac{A_1}{B_1}}\tan(m_1 x), \quad \tan(\theta_2(y)) = \sqrt{1 + \frac{A_2}{B_2}}\tan(m_2 y). \quad (15)$$

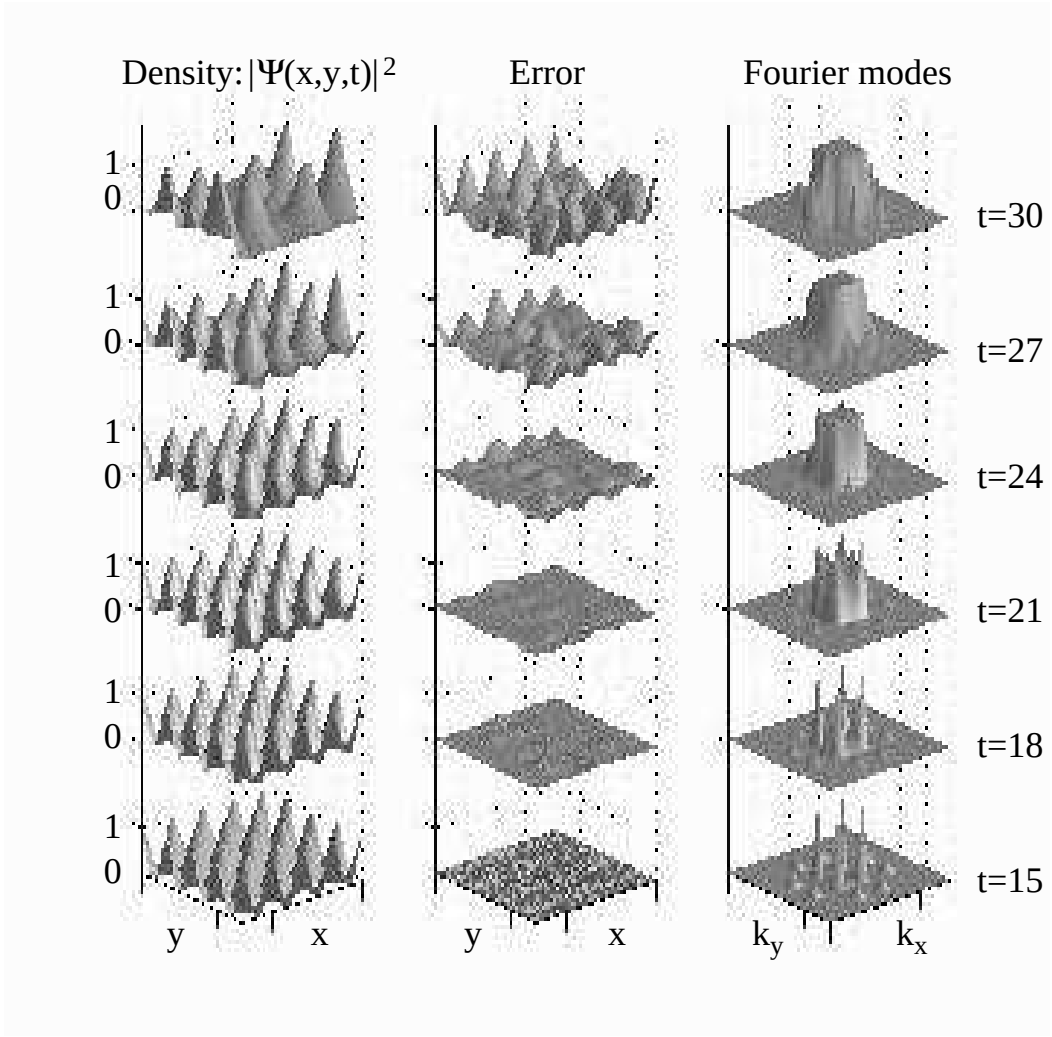

Fig. 4. A blow-up of the onset of instability occurring in Fig. 3. The middle figure shows $||\psi(x,y,t)|^2 - |\psi(x,y,t=0)|^2|$

.

These solutions are stable or unstable depending on the offset parameters B_1 and B_2. As shown in Fig. 2 the off-set $\mathrm{dn}(m_i x_i, k_i)$-type solution is stable whereas in Fig. 3 the unstable $\mathrm{sn}(m_i x_i, k_i)$ and $\mathrm{cn}(m_i x_i, k_i)$ solutions without offset are unstable. These trivial phase solutions suggest that offset is essential for stability. In Fig. 5, $A_1 = A_2 = 1$ and $B_1 = B_2 = 0.5$ and the onset of instability of the nontrivial phase solution is observed. Here the chosen offset ($B_1 = B_2 = 0.5$) is insufficient to stabilize the dynamics. In contrast, Fig. 6 has parameter values $A_1 = A_2 = 1$ and $B_1 = B_2 = 1$ and is stable. Thus with a higher offset, the nontrivial phase solution is stabilized. The boundary between the stable and unstable regions is difficult to calculate analytically and we rely on numerical simulations to determine the amount of offset required for stability. This behavior is again consistent with the one-dimensional case [11].

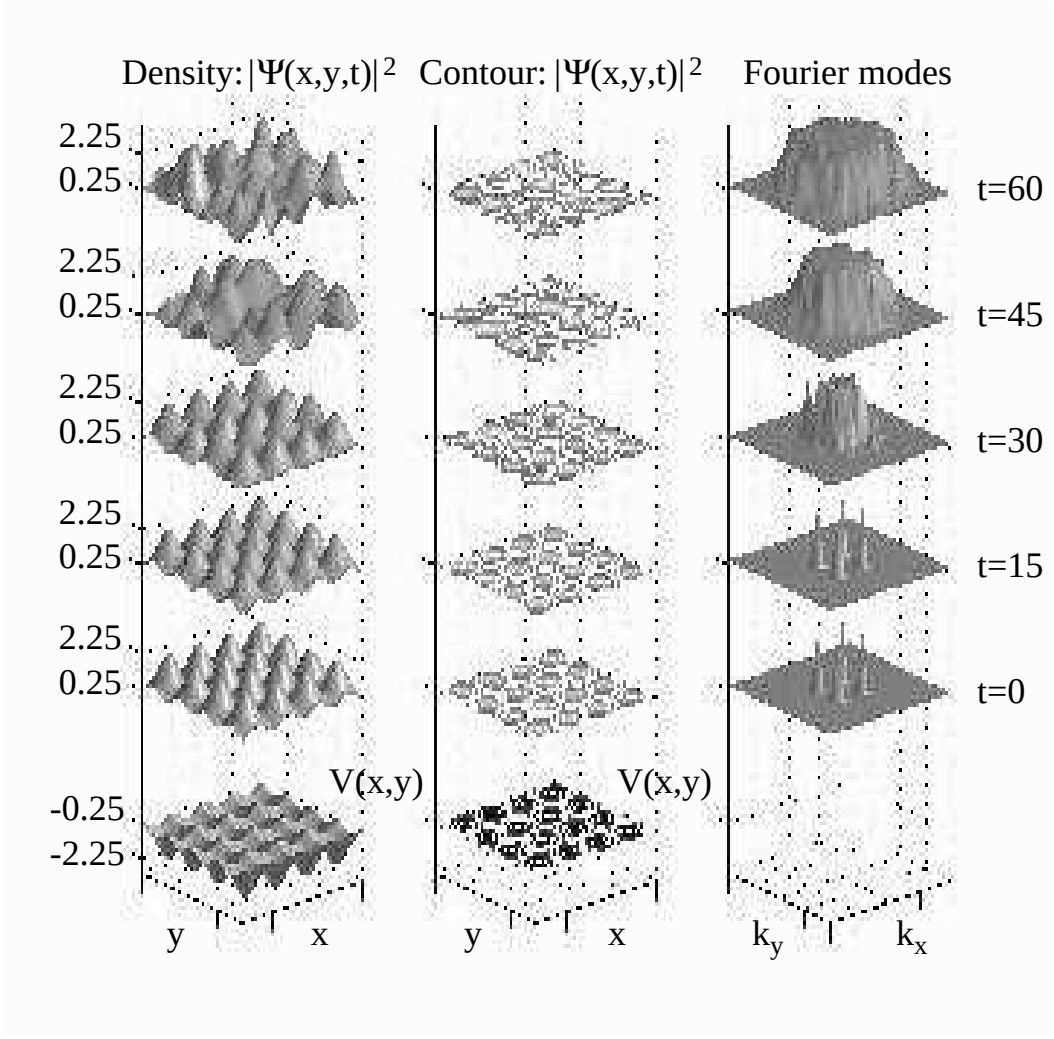

Fig. 5. An unstable solution from Eqns. (14) and (15). Here $k_1 = k_2 = 1/2$, $m_1 = m_2 = 1$, $A_1 = A_2 = 1$, and $B_1 = B_2 = 0.5$.

4 Summary and Conclusions

We considered the repulsive nonlinear Schrödinger equation with an elliptic function potential in two dimensions. Periodic solutions of this equation were found and their stability was investigated both analytically and numerically. Using analytical results for trivial-phase solutions, we showed that solutions with sufficient offset are linearly stable. This is confirmed with extensive numerical simulations on the governing nonlinear equation. Likewise, nontrivial-phase solutions are stable if they are sufficiently off-set.

Since our equations is a model for a Bose-Einstein condensate trapped in a lattice potential, our results imply that a large number of condensed atoms is sufficient to form a stable, periodic condensate. Physically, this implies sta-

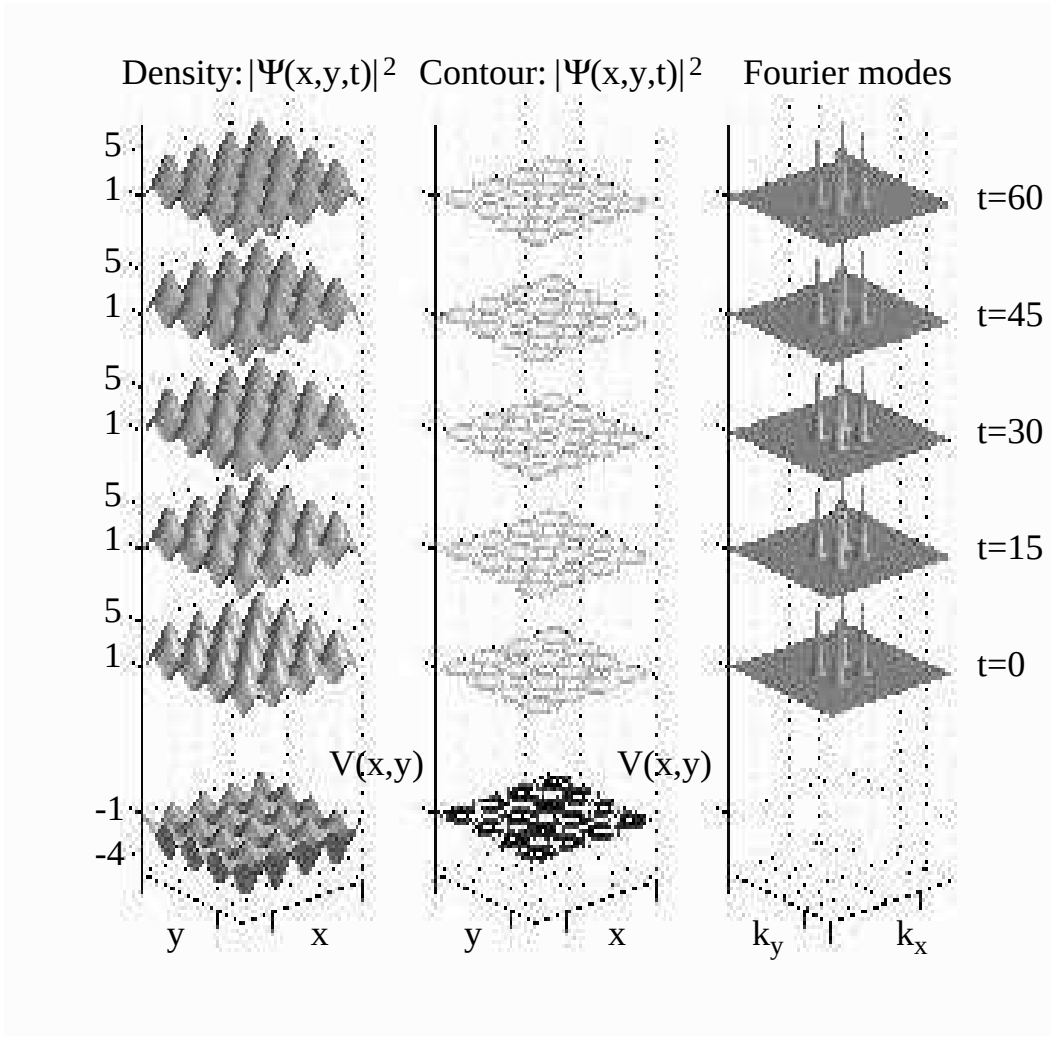

Fig. 6. A stable solution from Eqns. (14) and (15). Here $k_1 = k_2 = 1/2$, $m_1 = m_2 = 1$, $A_1 = A_2 = 1$, and $B_1 = B_2 = 1$.

bility of states near the Thomas–Fermi limit. The results are consistent with the one-dimensional trapping of a BEC condensate in a standing light wave. To quantify this phenomena, we consider the $k = 0$ limit and note that in the trigonometric limit $k \to 0$ the number of particles n per potential well is given by $n = \langle|\psi(x,y,t)|^2\rangle = \langle r_1^2(x)\rangle \langle r_2^2(y)\rangle = (A_1/2 + B_1)(A_2/2 + B_2)$, where $\langle\cdot\rangle$ denotes the spatial average. In the context of the BEC, and for a fixed atomic coupling strength, this means a large number of condensed atoms n per potential well is sufficient to provide an offset on the order of the potential strength. This ensures stabilization of the condensate. Alternatively, a condensate with a large enough number of atoms can be interpreted as a developed condensate for which the nonlinearity acts as a stabilizing mechanism.

Acknowledgments: The authors acknowledge useful conversations with J. C. Bronski, L. D. Carr, R. Carretero-González, K. Promislow, and W. Reinhardt.

References

[1] E. P. Gross. Structure of a quantized vortex in boson systems. *Nuovo Cimento*, 20:454–477, 1961.

[2] L. P. Pitaevskii. Vortex lines in an imperfect bose gas. *Sov. Phys. JETP*, 13:451–454, 1961.

[3] B. P. Anderson and M. A. Kasevich. Macroscopic quantum interference from atomic tunnel arrays. *Science*, 282:1686–89, 1998.

[4] E. W. Hagley, L. Deng, M. Kozuma, J. Wen, K. Helmerson, S. L. Rolston, and W. D. Phillips. A well-collimated quasi-continuous atom laser. *Science*, 283:1706–09, 1999.

[5] M. Kozuma, Y. Suzuki, T. Torii, Y. Sugiura, T. Kuga, E. W. Hagley, and L. Deng. Phase-coherent amplification of matter waves. *Science*, 286:2309–12, 1999.

[6] M. L. Chiofalo and M. P. Tosi. Output from Bose condensates in tunnel arrays: the role of mean-field interactions and of transverse confinement. *Phys. Lett. A*, 268:406–12, 2000.

[7] G. K. Brennen, C. M. Caves, P. S. Jessen, and I. H. Deutsch. Quantum logic gates in optical lattices. *Phys. Rev. Letters*, 82(5):1060–63, 1999.

[8] Y. B. Ovchinnikov, J. H. Müller, M. R. Doery, E. J. D. Vredenbregt, K. Helmerson, S. L. Rolston, and W. D. Phillips. Diffraction of a released Bose-Einstein condensate by a pulsed standing light wave. *Phys. Rev. Letters*, 83(2):284–87, 1999.

[9] D.-I. Choi and Q. Niu. Bose-Einstein condensates in an optical lattice. *Phys. Rev. Letters*, 82(10):2022–25, 1999.

[10] J. C. Bronski, L. D. Carr, B. Deconinck, and J. N. Kutz. Bose-Einstein condensates in standing waves: the cubic nonlinear Schrödinger equation with a periodic potential. *Phys. Rev. Lett.*, 2001. To appear; cond-mat/0007174.

[11] J. C. Bronski, L. D. Carr, B. Deconinck, and J. N. Kutz. Stability of repulsive Bose-Einstein condensates in a periodic potential. *Phys. Rev. E*, 2001. To appear; cond-mat/0010099.

[12] D. Jaksch, C. Bruder, J. I. Cirac, C. W. Gardiner, and P. Zoller. Cold bosonic atoms in optical lattices. *Phys. Rev. Letters*, 81(15):3108–11, 1998.

[13] C. Sulem and P.-L. Sulem. *The nonlinear Schrödinger equation: self-focusing and wave collapse*. Springer-Verlag, New York, 1999.